

Functional Electrospun Poly (Lactic Acid) Scaffolds for Biomedical Applications: Experimental Conditions, Degradation and Biocompatibility Study

Idalba A. Hidalgo A.^{*}, Felipe Sojo[†], Francisco Arvelo[†], Marcos A. Sabino^{*,‡}

Abstract: The electrospinning technique is a method used to produce nano and microfibers using the influence of electrostatic forces. Porous three dimensional networks of continuous and interconnected fibers as scaffolds were obtained from a poly (lactic acid) solution. The concentration of the polymeric solution, 12.5% m/w, as well as the conditions of voltage (V=11kV) and tip-metallic collector distance (H=13cm) were established to develop these scaffolds through the electrospinning process. The characteristics of the scaffolds, such as fiber diameter, sintering and the biomimetics of the characteristics of a native extra cellular matrix were verified by Scanning Electron Microscopy (SEM). The orientation induced in the material as a consequence of the electrospinning forces was studied by Differential Scanning Calorimetry (DSC) and X-Ray Diffraction (XRD). The same techniques were used to study the hydrolytic degradation of samples in a ringer solution (pH=7-7.4 at 37°C) for 12 weeks and showed evidences of superficial degradation on the microfibers. The suitability of these scaffolds for tissue engineering was studied through the primary cell culture of chondrocytes, by observing adhesion and cellular proliferation developed during 14 days of assay.

Keywords: electrospinning, scaffold, nano and microfibers, poly(lactic acid), biocompatibility, chondrocytes, tissue engineering.

1 Introduction

Micro and nanotechnology have become very interesting fields for scientists, engineers, doctors, pharmacologists, etc., and are considered as one of the priority

^{*} Group B⁵IDA, Department of Chemistry, Universidad Simón Bolívar, 89000, Caracas 1080-A, Venezuela.

[†] Institute of Experimental Biology (IBE), Universidad Central de Venezuela, 1041-A, Caracas, Venezuela. And Centro de Biociencias Fundación Instituto de Estudios Avanzados-IDEA, Valle de Sartenejas, Baruta-Miranda.

[‡] msabino@usb.ve (corresponding author)

investigation fields in many countries (1-5). Micro and nanofibers can be produced using different techniques such as: drawing, template synthesis, self-assembly, phase separation, bioextrusion, and electrospinning (1, 3, 4).

In particular, polymeric micro and nanofibers find several industrial applications (nano and microelectronic devices, electrostatic dissipation, etc.) in environmental engineering (liquid, gas, and molecular filtering), military clothing technology (minimum air impedance), in the field of cosmetics (skin cleansing and treatment by the use of medications), medicine and biomedical engineering (drug delivery devices, wound dressing, haemostatic devices, tissue engineering scaffolds, etc.) (1-7).

Tissue engineering is a discipline where knowledge on medicine, cellular biology, science and materials engineering, micro and nanotechnology, etc., has an enormous potential for the production of tissue substitutes as well as in helping in the clinical treatment of diseases associated to different human tissues and organs (6, 8,9).

Electrospinning has become the most popular and efficient method for the production of these type of fibers for tissue engineering applications, because it is possible to obtain fibers with submicrometric diameters (from nano to micro scale, also named “electrospun fibers”), which are at least one order of magnitude smaller than those obtained with other conventional fiber production techniques (3, 9, 10). The electrospinning equipment consists basically of a capillary tube (a syringe) containing the polymeric solution (or melt) with a small diameter needle, a metal collecting screen, and a high DC voltage source. Initially, one electrode or a DC wire is connected to the needle, and the collector may be simply grounded. Once the voltage supply starts, the polymeric solution is held by its surface tension forming a drop at the needle tip. As the voltage increases, the drop gets distorted because of the charge induced on the fluid surface, adopting a conic shape known as “Taylor cone”. Above a critical voltage, this surface tension is overcome and a polymer jet ejects from the Taylor cone, reducing its thickness until it reaches the metallic collector; the solvent evaporation occurs simultaneously. The result is a three-dimensional network of non-woven fibers arranged on the collector’s surface.

For a new tissue to be formed, the scaffold must have specific characteristics such as those observed in the micro/nanofibers obtained by electrospinning: a high surface/volume ratio, adjustable porosity, better mechanic performance than any other known form of material, and the possibility to conform different shapes and sizes (1,3,5,7,9,11,12).

For the last 10 years, there has been a growing interest in synthetic biodegradable polymers, particularly in poly(lactic acid)(PLA) and its copolymers (6,10,14,15),

due to their successful clinical use, not only in tissue engineering scaffolding, but also in reabsorbable sutures and drug delivery devices (6,7,8,9,14,15). Besides, PLA has the Food and Drug Administration certification for clinical use (6).

This research has been focused on the production of scaffolds (using a neat amorphous PLA) for tissue engineering purposes using electrospinning. The aim of this research is to relate the molecular orientation of the electrospun fibers with the experimental conditions of production of these PLA scaffolds, as well as to show the way how this orientation affects the hydrolytic degradation process. Furthermore a biocompatibility study using a primary cell culture of chondrocytes was carried out.

2 Materials and Methods

2.1 Fabrication of PLA Scaffolds

Polymer solutions were prepared by dissolving the PLA ($M_w \approx 1.5 \times 10^5$, Ingeo Biopolymer 3001D, Nature Works) in chloroform (Merck Chemicals), at concentrations of 20, 15, 12.5, and 10% w/v. Four mlml of each concentration of the polymer solution were added to a 10-ml glass syringe. Needles of 18-G with a 1.2 mm inner diameter were used. The distance between the syringe needle tip and the aluminum collector was adjusted to 22, 19, 16, and 13 cm. A high voltage of 6, 8, 11, and 12.5 kV was applied using a voltage regulated DC power supply to generate the polymer jet.

2.2 Morphology of PLA Scaffolds

The morphology of PLA scaffolds was studied using a scanning electron microscopy SEM (Jeol JSM 6390 equipment). Before the scaffold samples were observed, they were coated with gold using a sputter coater (Balzers). A voltage of 25 kV was used and the fiber diameter was measured from SEM micrographs using free software.

2.3 Induced Orientation, DRX and DSC Analysis

As the electrospinning process induced a molecular orientation of the polymer, we used wide angle X-ray diffraction analysis (XRD) to study fiber orientation, using the samples obtained under optimum process conditions = 12.5%w/w, 11 kV, 13 cm. A PLA film obtained by solvent casting was measured as a reference.

We used a DSC-7 (Perkin Elmer) to study the samples by Differential Scanning Calorimetry(DSC). Five-mg samples were hermetically sealed in aluminum pans, which were then subjected to a heating-cooling-heating dynamic cycle at 20°C/min (from 0°C to 200°C). This cycle was used for orientation and hydrolytic degradation studies as well.

2.4 Controlled Hydrolytic Degradation

Commercial ringer solution, pH = 7.4, was used to promote the hydrolytic degradation of the scaffold samples in falcon tubes, placed in a “bain-marie” at 37 °C (Boekel water bath $\pm 1^\circ\text{C}$). The degradation time was 8 weeks. A PLA film was used as a control.

2.5 Cell Culture and Seeding

Cartilage chondrocytes were dissected from a human nasal cartilage sample obtained from the Institute of Experimental Biology (IBE, Universidad Central de Venezuela, considering ethical protocols). Cells were cultured in a medium (Ham F12 Gibco), supplemented with 10% bovine fetal serum, 1% antimycotic-antibiotic, 50 $\mu\text{g}/\text{mL}$ of ascorbic acid. The viable cell number was determined using a Neubauer chamber.

From collected cells, 5000 cells/ml were suspended in the culture supplemented medium seeded in a 9.6 cm^2 flask and cultured under a 5% CO_2 atmosphere at 37 °C. After achieving confluence, the flasks were washed three times with PBS and then treated with trypsin (1 \times). The cells were subcultured onto 3 samples of each PLA scaffold placed indifferent 6-well plates: 1×10^4 , 3×10^4 , and 5×10^4 cells. The scaffold samples were previously sterilized using a dilute ethanol solution and PBS, and placed for 15 min under a UV lamp. Samples were cultured under the described conditions for 14 days. Then, cells were observed with an optical microscope (IX50 Olympus) and were analyzed with integrated image software.

3 Results

3.1 Production and Morphology Analysis of PLA Scaffolds

The processing parameters used to prepare electrospun PLA scaffolds were optimized. We found an important dependence of both the morphological scaffold properties and the starting of the process itself on the concentration of the polymeric solution (viscosity). First of all, electrospinning is considered as a “one-step” technique, so parameters involving the obstruction of the process (such as needle blockage) were eliminated. Macroscopically, the target was to obtain a consistent and continuous mesh or film, without excess of surface drops, easily removable from the metallic collector, and preserving the physical integrity of the product after the removal. Samples complying with these conditions were analyzed by SEM. According to the results, the optimum processing conditions finally were: a 12.5% w/v PLA solution, an 11 kV voltage (V), and a 13 cm needle to collector distance (H). Figure 1 shows a SEM photography of a scaffold sample obtained under these

conditions:

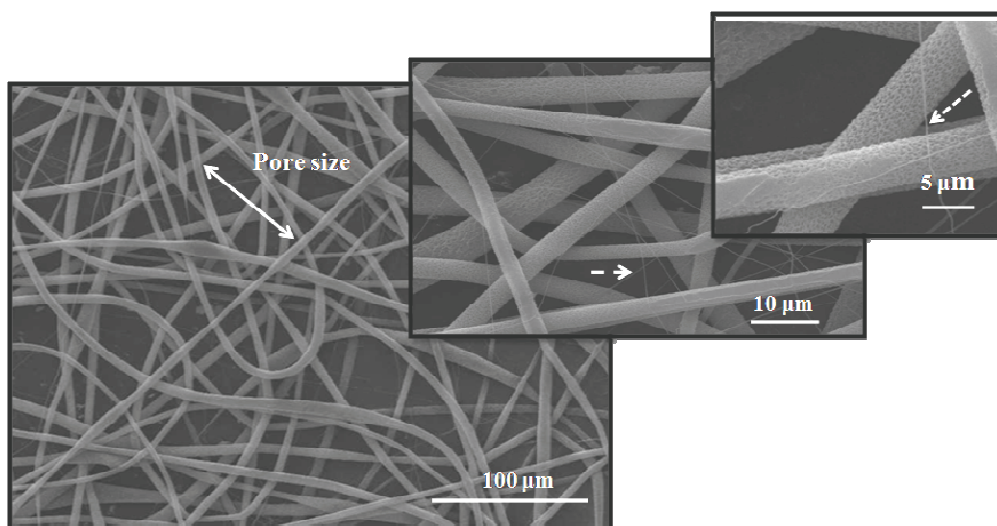


Figure 1: PLA scaffold produced under optimum processing conditions: 12.5% w/v, 11 kV, 13 cm. In upper micrograph a pore in the mesh is detailed. Dotted arrows indicate the presence of some nanofibers in the scaffold.

Figure 1 exhibits a nano/microfibrous scaffold, showing continuous filaments with consistent diameters along their extension, in general; a porous mesh surface forming a three-dimensional network with an average diameter of $8.10 \pm 0.06 \mu\text{m}$ and an average pore size of $82.9 \pm 0.9 \mu\text{m}$ is also evident.

By SEM analysis, it has been possible to observe that the surface of the fibers is porous (Figure 2), a feature present in all samples studied and produced under different processing conditions.

Details of topography along the surface of the fibers. Nano fibers are also observed.

Several previous works show electrospun fibers based on PLA exhibiting similar characteristics as those observed in Figure 2. Luo et al. (2002) (16) considered that the vapor pressure of the polymeric solution used had a critical influence on the formation of these surface pores. They reported that using a solvent with a low vapor pressure (low volatility) produced a decrease in such topography-porosity. In this case, however, chloroform has a high volatility rate (vapor pressure, $V_p=156 \text{ mmHg}$ (3)), so its evaporation may then be responsible for this surface roughness of the microfiber (3, 16, 17).

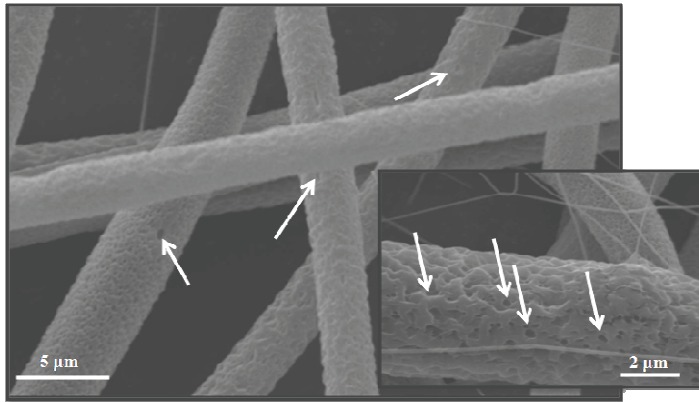


Figure 2: SEM micrographs of a PLA scaffold (12.5%*m/w*, 10 kV, 13 cm).

During the electrospinning process, the charged solution jet accelerates towards the metallic collector and elongates at a very high rate. As this occurs, the surface area of the jet is increased and causes an increase in the rate of solvent evaporation. A thermodynamic instability occurs during the loss of solvent and results in a phase separation within the electrospun fibers and the electrospun solution phase, generating this topography. Once the mesh is on the collector, the solvent-rich phase could form surface pores during the final drying of the fibers. Such topography is considered suitable for tissue engineering developments, because this porosity could promote a subsequent degradation process, as well as the cellular adhesion and proliferation (18).

A scaffold for tissue engineering purposes must mimic the native extra cellular matrix(3, 7, 8, 9) being a consistent three-dimensional network of interconnected and sintered fibers, with a suitable pore size distribution, so that the scaffold would not obstruct the cellular infiltration, a requirement that could be satisfied by combining the advantages of nano and microfiber scaffolds.

A cryogenic fracture of a scaffold sample was analyzed by SEM in order to verify the fibers interconnectivity and sintering. Figure 3 shows a three-dimensional PLA scaffold, exhibiting a mesh of connected nano and microfibers, with sintering zones identified with arrows:

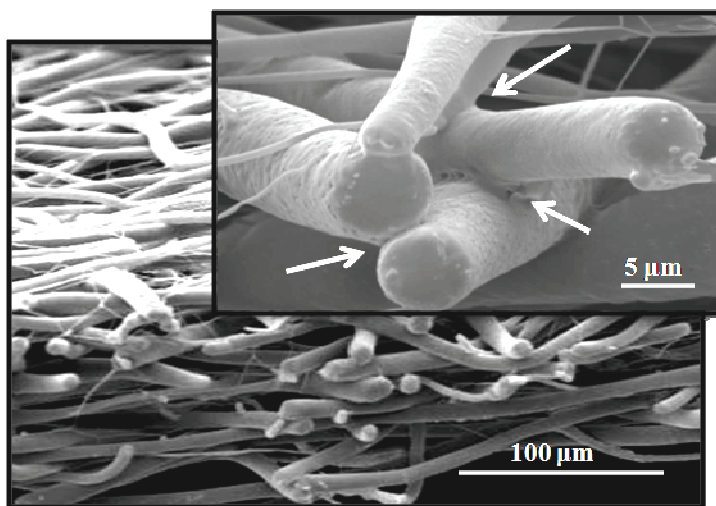


Figure 3: SEM micrographs showing the fibers interconnectivity and sintering, forming a three-dimensional porous network.

3.2 Molecular Induced Orientation by Electrospinning

3.2.1 Wide Angle X-ray Diffraction (WAXD)

2D WAXD studies were made to analyze the molecular orientation effect induced in electrospun fibers. Figure 4 shows the diffraction pattern of an amorphous PLA film, produced by solvent casting from the 12.5% w/v PLA solution.

The figure shows a diffraction pattern corresponding to an amorphous polymeric material: the absence of sharp, well-defined peaks and the presence of an amorphous halo, which contrasts with the figure below (Figure 5), where the peaks at approximately $2\theta=16.4^\circ$ and 18.7° adjust to those previously reported for the alpha (α) form of PLLA crystals having a pseudo-orthorhombic unit cell (19).

Some researchers (3,18, 19, 20, 21) mentioned that although the polymer chains are non-crystalline in the fibers, they could be highly oriented. Similar results, meta stable states of highly oriented, but non-crystalline chains, located between the amorphous and crystalline states, have been reported in other electrospinning studies based on other polymeric materials such as isotactic polypropylene (iPP), Kevlar, poly(ethylene) oxide (PEO), poly(acrylonitrile) (PAN), and Nylon 6. This phenomenon is attributed to the rapid solidification of stretched chains at the high rates of elongation during the process, which inhibits the formation of the crystals. The chains do not have time enough to organize into a suitable crystalline form

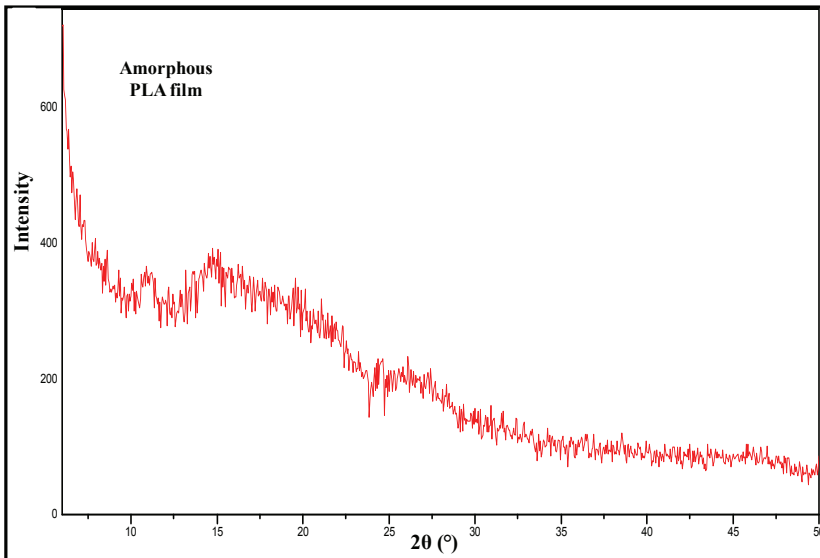


Figure 4: WAXD pattern of an amorphous PLA film (produced by solvent casting)

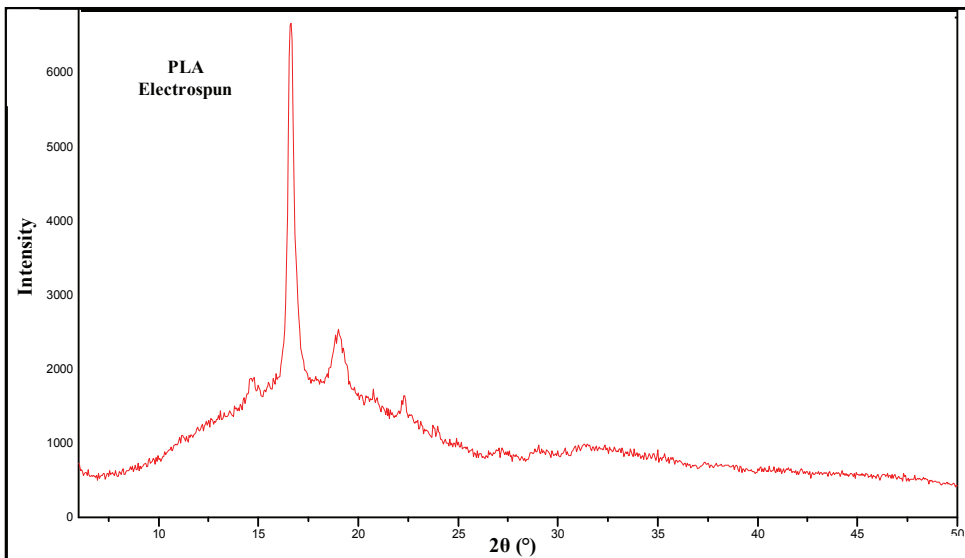


Figure 5: WAXD pattern of electrospun PLA scaffold produced under optimum processing conditions (12.5%*m/w*, 11 kV, 13 cm)

before their solidification, but are well oriented.

In an electrospinning process, the jet ejects from the needle tip and the polymeric chains stretch along the direction of the electrostatic field. The solvent starts to evaporate in a very short time. This solidification process reduces chain mobility, and the degree of crystallinity of the electrospun fibers is lower than that of the material in its previous form before the electrospinning process (if it is based on an initially semi-crystalline polymer). Therefore, the solvents with lower evaporation rates give the chains more time to arrange, allowing the development of highly oriented structures (18) even in the case of amorphous polymers.

3.2.2 Differential Scanning Calorimetry (DSC)

DSC studies were made in order to compare the thermograms of the amorphous PLA film (obtained by solvent casting), and those of the electrospun PLA scaffolds obtained by different voltages. DSC results could give information about the molecular induced orientation in PLA, and establish relations between the degree of crystallinity reached and the different voltages used in the electrospinning process. Figure 6 shows the DSC thermograms of the electrospun PLA scaffolds produced using the 12.5% w/v PLA solution, a $H = 13$ cm needle to collector distance, and $V = 6, 8$ and 11 kV voltages:

When comparing the first heating curves obtained from the PLA film and the electrospun scaffolds, a cold-crystallization process is evidently present in the DSC thermograms. There can also be seen a phenomenon at low crystallization rates, which may indicate that the oriented material with meta stable crystalline structures has invested the heating energy in its rearrangement and cold-crystallization. This is a contrast to what was observed in the heating thermogram of the highly amorphous PLA film, in which the cold-crystallization process is hindered.

The comparison of the melting points in all thermograms allowed to corroborate that the electrospun samples had more developed crystalline or oriented structures, which needed more thermal energy to melt than those few crystalline structures with smaller lamellar thickness present in the amorphous PLA film. It is then evident that electrospun fibers do crystallize (based on the degree of crystallinity, χ_c), probably because polymeric chains align as a result of the extrusion through the needle, due to the generated electrostatic forces. Thermal transitions and other parameters from the DSC thermograms from Figure 6 are shown in Table 1:

The results show that a higher crystallinity was reached when using 6 and 8 kV instead of 11 kV in the electrospinning process. This behavior is related to the results reported by Ramakrishna et al (2005) (3) who established that fiber crystallinity is affected by the effect of the electrostatic field, and the available time to crystallize

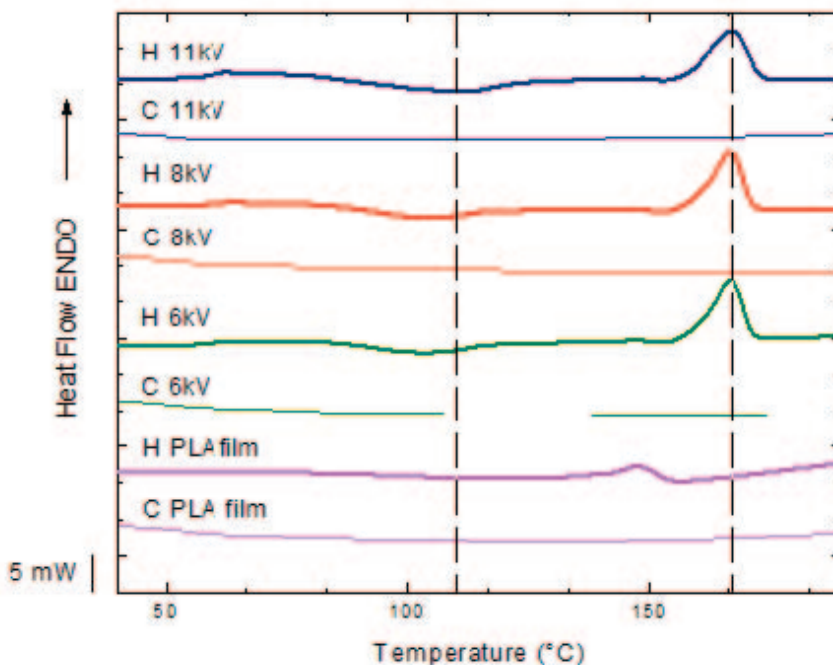


Figure 6: DSC thermograms: first heating (H) and cooling (C) of scaffolds produced by electrospinning: 12.5% w/v, 13 cm, and 6, 8, 11 Kv. As a reference, the H and C thermograms of amorphous PLA film are included at the bottom of the figure.

during the travel of the polymeric jet towards the metallic collector. A voltage increase leads to less flight time of the polymeric solution, as well as less time to crystallize.

The crystallinity percentage (χ_c) reached was not significantly different for the three electrospun samples, even though the orientation obtained for the 11 kV electrospun sample should have been the lowest; however, this was not determinant in the χ_c reached. It is possible that the induced orientation was enough to increase the χ_c (similar to the 6 and 8 kV samples) in addition to the thermal energy provided during the DSC heating. A hypothesis to be shown in future work can be proposed: it is possible that the material could have degraded because of the high electric field generated at 11 kV, producing an increase in polymer chain polydispersity, *i.e.*, the presence of chains of different molecular weight results in the enlargement of the cold-crystallization temperature range, and, consequently, chain entanglements.

Table 1: Thermal transitions: glass transition temperature, cold-crystallization temperature, and melting point (T_g , T_c , $T_m \pm 0.5^\circ\text{C}$), crystallization and fusion enthalpy (ΔH_c , $\Delta H_f \pm 10\%$) of electrospun samples.

Sample	6 kV	8 kV	11 kV	PLA film
T_g ($^\circ\text{C}$)	60.2	59,4	58.5	49.7
T_{c1} ($^\circ\text{C}$)	103.7	103.7	111.1	-
T_{c2} ($^\circ\text{C}$)	153.1	153.1	153.1	-
T_m ($^\circ\text{C}$)	167.1	167.1	167.1	147.4
ΔH_c (J/g)	24	22	29	-
ΔH_f (J/g)	33	33	34	9
$\Delta H_f - \Delta H_c$ (J/g)	9	12	5	-
χ_c (%)	36	34	37	-

3.3 Hydrolytic Degradation Assay

A PLA film obtained by solvent casting and samples of a scaffold produced under optimum processing conditions were studied during 12 weeks under the hydrolytic degradation conditions described in experimental section.

The human physiological environment has suitable conditions to promote the development of hydrolytic processes (22,23). In this sense, a polymer such as PLA should have hydrolytically unstable bonds for biodegradation to occur in an ideal period of time and under physiological pH conditions (7-7.4 at 37°C).

There are several factors to consider when studying the hydrolytic degradation: the characteristics of the reaction medium (temperature, compounds present, pH, etc.), relative humidity, chemical structures and polymer crystallinity, etc. (23, 24). The larger the proportion of amorphous zones in the system, the easier the diffusion of the solution or reaction medium, and, consequently, polymer degradation (23-25).

Figure 7 shows the DSC thermograms of the first heating of the PLA film samples after the hydrolytic degradation. An annealing process seems to have occurred from week 0 to week 8, with an increase in the crystallinity χ_c : 13 % (week 0), 24 % (week 4), and 30% (week 8). The efficiency of the degradation process could become more evident when comparing the changes from week 8 to 12, where T_g values are considered and fusion enthalpy and crystallinity percentage increased (see Table 2):

Figure 8 shows the DSC thermograms obtained for the electrospun PLA scaffold produced under optimum processing conditions after a hydrolytic degradation process for up to 12 weeks.

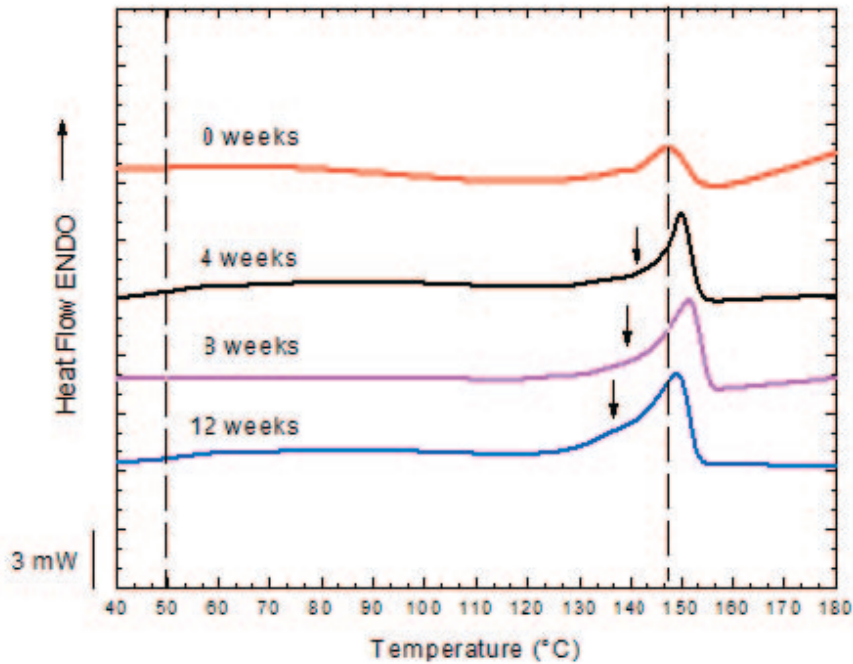


Figure 7: DSC first heating of PLA films after hydrolytic degradation in ringer solution at 37°C for up to 12 weeks.

Table 2: PLA film properties: thermal transitions: glass transition temperature, and melting point (T_g , $T_m \pm 1^\circ\text{C}$), fusion enthalpy ($\Delta H_f \pm 10\%$), submitted to hydrolytic degradation for 12 weeks.

Sample	Film-week 0	Film-week 4	Film-week 8	Film-week 12
T_g ($^\circ\text{C}$)	49.7	52.2	54.6	51.3
T_m ($^\circ\text{C}$)	147.4	150.0	151.7	149.0
ΔH_f (J/g)	12	23	28	31
χ_c (%)	13	24	30	34

The thermogram of the scaffolds after week 4 in Figure 8 shows an aging peak that could be attributed to a rearrangement process at the amorphous zone of the material promoted by the increase of the temperature (test temperature). This behavior is consistent with the first stage of the degradation process, where crystalline zones have not yet been attacked (26, 27,28).

Between week 4 and week 8, the increase in crystallinity and fusion enthalpy

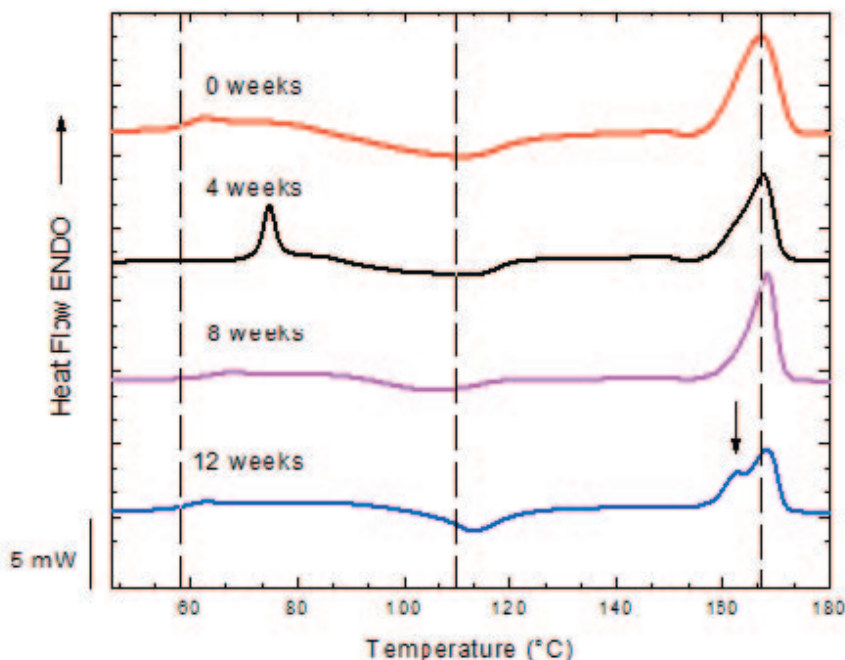


Figure 8: DSC first heating of PLA scaffolds after hydrolytic degradation in ringer solution at 37°C for up to 12 weeks.

(see Table 3) could be a consequence of the chains arrangement resulting from the molecular changes that occurred in the amorphous zones which allow for the formation of crystalline species of different molecular sizes. This effect is even more evident when comparing changes from week 8 to week 12, where T_g and T_c decrease, indicating the presence of low molecular weight chains that could crystallize at lower temperatures.

It can be verified that the degradation occurred, but it cannot be established if the crystalline zones of the material have been effectively affected, because the melting point has not changed at week 12. A severe attack to the crystalline zones would also involve the progressive decrease of the percentage of crystallinity after reaching a peak point during the degradation exposure time. Therefore, it is supposed that the degradation time should be longer to reach such effects..

Table 3: PLA scaffold properties:thermal transitions: glass transition temperature, cold crystallization temperature and melting point (T_g , $T_m \pm 1^\circ\text{C}$), crystallization and fusion enthalpy ($\Delta H_f \pm 10\%$), exposed to hydrolytic degradation for 12 weeks.

Sample	11 kV-week 0	11 kV-week 4	11 kV-week 8	11 kV-week12
T_g ($^\circ\text{C}$)	58.5	~ 74	62.1	59.3
T_c ($^\circ\text{C}$)	111.1	112.7	105.0	103.3
T_m ($^\circ\text{C}$)	167.1	167.7	168.3	167.7
ΔH_c (J/g)	29	27	20	16
ΔH_f (J/g)	34	35	36	34
χ_c (%)	37	38	38	36

3.4 Cell Culture and Seeding

Human chondrocytes were obtained from fragments of human nasal cartilage processed mechanically and enzymatically as described in the experimental protocol, and seeded on PLA scaffold samples (produced under optimum processing conditions 12.5 % w/v, 11 kV, 13 cm). These samples were incubated under the temperature and atmosphere conditions described in the experimental protocol and were observed under an optical microscope after 48 hrs, 7, and 14 days of culture,.

It is clear in the micrographs (Figure 9) that cells are well distributed around the fiber mesh and probably in the first stage of the cell adhesion process. The topography of PLA fibers, evidenced in figure 2, also could be responsible for this cell behavior, as well as the electrical static charge induced for the electrospinning process on the surface of electrospun fibers.

Figures 10 and 11 below show the cultures after 14 days of incubation observed with the optical microscope when 3×10^4 and 5×10^4 cells were seeded (compare with figure 9(b) and 9(c)).

In Figures 10 and 11, the dark zones highlighted by asterisks correspond to chondrocyte aggregation embedded in the scaffold. They are observed below the superficial fibers shown in the micrographs, in the upper left of each figure. As reported in the literature it is necessary that chondrocytes cell are embedded in the 3D structure, because they don't adopt a fibroblastic shape (i.e. cellular de differentiation process) (29).

After 14 days of culture, it could be considered that a cellular migration occurred through the fibrous scaffold. Compared with the results at the initial adhesion time (except for the lower cell density 1×10^4 cells, where cell proliferation was not observed), the cellular proliferation was better when a high cell concentration was seeded (3×10^4 cells or 5×10^4 cells) onto the electrospun scaffold, even more than

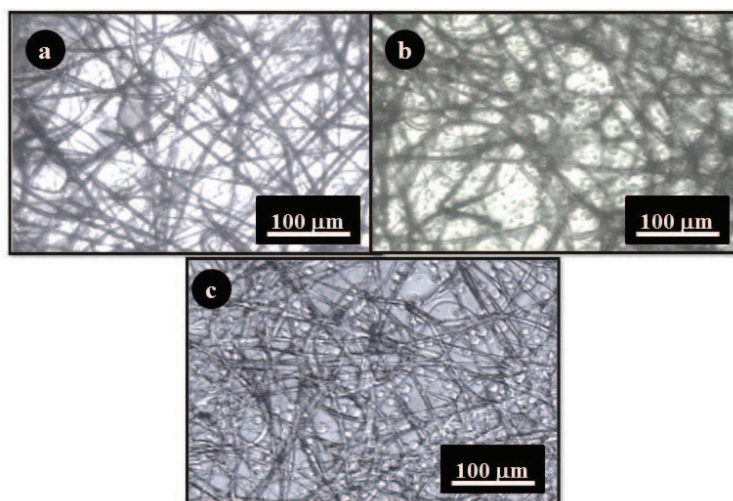


Figure 9: Optical micrographs of scaffold samples after 4hrs of cellular culture: Electrospun PLA Scaffold, seeded a) 1×10^4 cells, b) 3×10^4 cells, c) 5×10^4 cells.

in the case of the control sample (PLA film). Additionally, all the cells cover the fiber surface on the electrospun scaffold cells, and then they can migrate under the fibers through the porous scaffold structure, indicating that scaffolds obtained by electrospinning are suitable for cellular growth (proliferation, migration and differentiation (29)) and tissue engineering.

The initial number of cells seeded was 3×10^4 . The micrograph shows the cell morphology and aggregation.

Jin et al. (2005) (30) studied the proliferation of fibroblasts on electrospun scaffolds and film-type scaffolds, using PLASB, poly (L-lactic acid-co-succinic acid-co-1, 4-butanediol), and found that seeded cells could get lost through the electrospun scaffold pores. This explained the difference in cellular density reported at the beginning of the culture assay between the electrospun scaffold samples and the film-type scaffold.

To verify this evidence on figure 10, the cellular proliferation in the PLA electrospun scaffold samples was determined as compared with the initial cells seeded on the mesh (Figure 11).

The initial number of cells seeded was 5×10^4 . The micrograph shows the cell morphology and chondrocyte aggregation.

According to this result, it is assumed that the higher the amount of cells seeded, the higher the probability of reaching a high level of attached cells, and also the

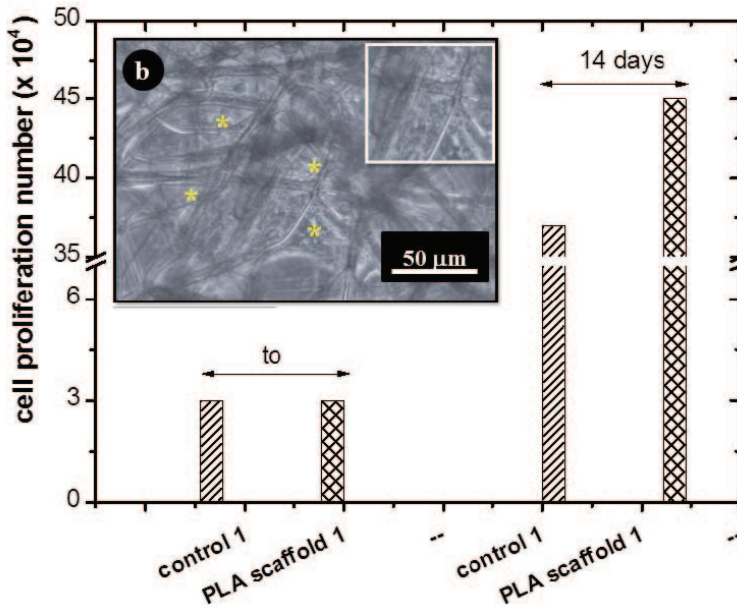


Figure 10: Micrographs of PLA scaffolds after 14 days of cellular culture.

higher the proliferation. Accordingly, Chaim et al. (2011) (29) concluded that the greater the number of adherent cells, the greater the resulting proliferation. Li et al. (2003) (31), verified their suitability for the proliferation of bovine fetal chondrocytes through the study with electrospun PCL scaffolds. In addition to their studies related to cytocompatibility of scaffolds, they reported the potential of fibrous scaffolds to reach and maintain the chondrogenic differentiation effect also observed in this study using PLA scaffolds produced by electrospinning.

4 Conclusions

The electrospinning technique involves a meticulous selection of processing parameters, as well as the materials to be used, as they influence the morphology and the characteristics of the scaffold. The applied voltage, the needle to collector distance and, concerning the material system used, the concentration of the polymeric solution, are the most influential processing parameters.

MEB analysis allowed the selection of the optimum processing parameters for the production of PLA scaffolds: 12,5 % w/v polymer solution, V = 11 kV and H = 13 cm.

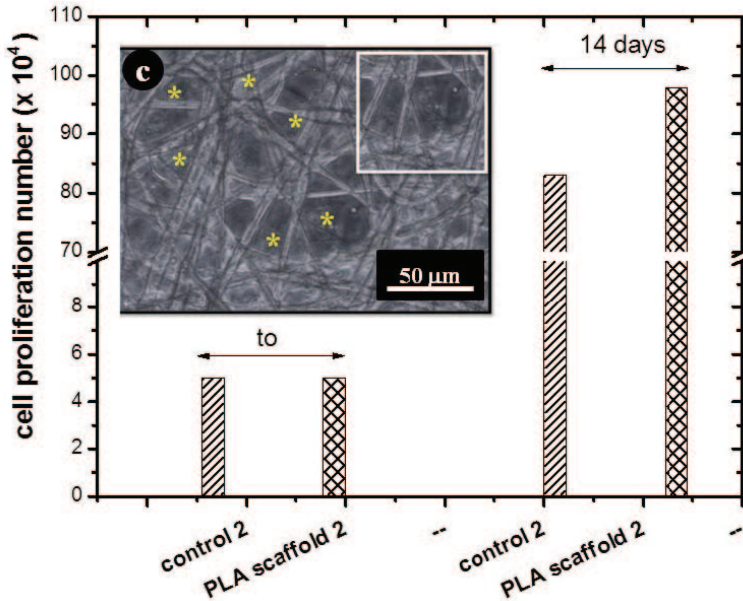


Figure 11: Micrographs of PLA scaffolds after 14 days of cellular culture.

As a result of the electrostatic forces in the system, the polarization induced in the material, and the extrusion of the polymeric solution through the needle, the electrospinning process imparts molecular orientation to the material which depending on the flight time towards the metallic collector. The vapor pressure of the solvent used also is responsible for the topography of the fiber.

The oriented polymer chains could arrange into crystalline structures with metastable characteristics. Using X-ray diffraction and DSC analysis, it was possible to verify a higher orientation and crystallinity in scaffolds produced by applying 11 kV and a 13 cm needle to collector distance.

PLA scaffold samples under hydrolytic degradation at 37°C, during a 12 week assay, showed that PLA suffered a process of molecular rearrangement caused by the effect of the provided temperature. Evidence of the onset of a degradation process was also obtained by using DSC analysis.

The biocompatibility results given by chondrocytes culture seeding on electrospun PLA scaffolds allowed confirming the suitability of these electrospun fibers to allow adhesion and promote cellular proliferation by acting as a biomimetic extracellular matrix. Cellular viability was verified after 2 weeks of test. It was also possible to favor the chondrocytes differentiated state, a fundamental aspect to guarantee

a normal tissue development.

Acknowledgement: Authors wish to gratefully acknowledge the High Voltage Laboratory (LAB A-USB) for collaborate for the electrospinning tests. They would also like to thank the Polymer Group (GPUSB) for the DSC analysis, and the Surface Laboratory (LAB E-USB) for the SEM analysis.

References

1. Huang Z-M., Zhang, Y.-Z., Kotaki, M., Ramakrishna, S., "A review on polymer nanofibers by electrospinning and their applications in nanocomposites", *Composites Science and Technology*, Vol. 63, 2003, pp.2223-2253.
2. Kowaleswsky, T. A., Blonski, S., Barrel, S., "Experiments and modeling of electrospinning process", *Bulletin of the Polish Academy of Sciences*, Vol. 53, 2005, pp.385-394.
3. Ramakrishna, S. Fujihara, K., Teo, W-E., Lim, T-C., Ma, Z. "An Introduction to Electrospinning and Nanofibers", World Scientific, 2005.
4. Ma, P. X., "Biomimetic materials for tissue engineering", *Advanced Drug Delivery Reviews*, Vol. 60, 2008, pp. 184-198.
5. Piperno, S., Lozzi, L., Rastelli, R., Passacantando, M., Santucci, S., "PMMA nanofibers production by electrospinning", *Applied Surface Science*, Vol. 252, 2006, pp. 5583-5586.
6. Wnek-G, Bowlin, L., "Encyclopedia of Biomaterials and Biomedical Engineering", Marcel Dekker, Nueva York, EE.UU, 2004, pp. 543-549, 737-739, 1663-1669.
7. Liang, D., Hsiao, B. S, Chu, B., "Functional electrospun nanofibrous scaffolds for biomedical applications", *Advanced Drug Delivery Reviews*, Vol. 59, 2007, pp. 1392-1412.
8. Pallua, N., Suscheck., C., "Tissue Engineering: From Lab to Clinic", Springer, Germany, 2011.
9. Saltzman, W. M., "Tissue Engineering: engineering principles for the design of replacement organs and tissues", Oxford University Press, Inc., Nueva York, EE.UU., 2004.

10. Ray, S. S., Bousmina, M., "Biodegradable polymers and their layered silicate nanocomposites: In greening the 21st century materials world", *Progress in Materials Science*, Vol. 50, 2005, pp. 962-1079.
11. Milleret, V., Simona, B., Neuenschwander, P., Hall, H., "Tuning electrospinning parameters for production of 3D-fiber-fleeces with increased porosity for soft tissue engineering applications", *European Cells and Materials*, Vol. 21, 2011, pp. 286-303.
12. Bhardwaj, N.; Kundu, S. "Electrospinning: A fascinating fiber fabrication technique", *Biotechnology Advances*, Vol. 28, 2010, pp. 325-347.
13. Lim, L-T., Auras, R., Rubino, M., "Processing technologies for poly(lactic acid)", *Progress in Polymer Science*", Vol. 33, No. 8, 2008, pp. 820-852.
14. Torres-Giner, S., Gimeno-Alcñiz, J. V., Ocio, M., Lagaron, J. M., "Optimization of Electrospun Polylactide-Based Ultrathin Fibers for Osteoconductive Bone Scaffolds", *Journal of Applied Polymer Science*, Vol. 122, No. 2, 2011, pp. 914-925.
15. Gupta, A. P., Kumar, V., "New emerging trends in synthetic biodegradable polymers-Polylactide: A critique", *European Polymer Journal*, Vol. 43, 2007, pp. 4053-4074.
16. Luo, C.J., Nangrejo, M., Edirisinghe, M., "A novel method of selecting solvents for polymer electrospinning", *Polymer*, Vol. 51, No. 7, 2010, pp. 1654-1662.
17. Bognitzky, M., Czado, W., Frese, T., Schaper, A., Hellwig, M., Steinhart, M., Greinier, A., Wendorff, J., "Nanostructured fibers via electrospinning", *Advanced Materials*, Vol. 13, 2001, pp. 637-640.
18. Asran, A.Sh., Salama, M., Popescu, C., Michler, G.H., "Solvent influences the morphology and mechanical properties of electrospun poly(L-lactic acid) scaffold for tissue engineering applications", *Macromolecular Symposia*, Vol. 294, No. 1, 2010, pp. 153-161.
19. Zong, X., Kim, K., Fang, D., Ran, S., Hsiao, B.S., Chu, B., "Structure and process relationship of electrospun bioabsorbable nanofiber membranes", *Polymer*, Vol. 43, 2002, pp. 4403-4412.
20. Cho, A-R., Shin, D.M., Jung, H.W., Hyun, J.C., Lee, J.S., "Effect of Annealing on the Crystallization and Properties of Electrospun Polylactic Acid and

- Nylon 6 Fibers”, *Journal of Applied Polymer Science*, Vol. 120, 2010, pp. 752-758.
21. Garg, K., Bowlin, G., “Electrospinning jets and nanofibrous structures”, *Biomicrofluidics*, Vol. 5, 2011, pp. 13403-19.
 22. Andrady, A., “Science and Technology of polymer nanofibers”, Wiley, Nueva Jersey, EE.UU., 2008.
 23. Sabino, M.A., Morales, D., Ronca, G., Feijoo, J.L., “Study of hydrolytic degradation of a biodegradable copolymer” (in Spanish) *Acta Científica Venezolana*, Vol. 54, 2003, pp. 18-27.
 24. Brito, Y., Sabino, M.A., Ronca, G., Muller A.J. “Changes in Crystalline Morphology, Thermal, and Mechanical Properties with Hydrolytic Degradation of Immiscible Biodegradable PPDx/PCL Blends”. *Journal of Applied Polymer Science*, Vol 110, 2008, pp. 3848–3858.
 25. Chu, C.C., Campbell, N.D., “Scanning electron microscopy study of the hydrolytic degradation of poly(glycolic acid) suture”, *Journal of Biomedical Materials Research*, Vol. 16, 1982, pp. 417-430.
 26. Lorenzo, T. Sabino, M.A., Müller, A.J., “Biodegradation study of a polyblend poly(ϵ -caprolactone)/cornstarch (PCL/ALM) and its compatibility with plasticized starch” (in Spanish) *Revista Latinoamericana de Metalurgia y Materiales*, Vol. 23, No. 2, 2003, pp. 25-35.
 27. Sabino, M.A., Albuerne, J., Müller, A.J., Brisson, J., Prud’homme, R., “Influence of in Vitro Hydrolytic Degradation on the Morphology and Crystallization Behavior of Poly(p-dioxanone)”, *Biomacromolecules*, Vol. 5, 2004, pp. 358-370.
 28. Sabino, M.A., González, S., Márquez, L., Feijoo, J.L., “Study of the hydrolytic degradation of polydioxanone PPDx”, *Polymer Degradation and Stability*, Vol. 69, 2000, pp. 209-216.
 29. Chaim, I.A., Sabino, M.A., Mendt, M., Müller, A.J., Ajami, D., “Evaluation of the potential of novel PCL-PPDX biodegradable scaffolds as support materials for cartilage tissue engineering”, *Journal of Tissue Engineering and Regenerative Medicine*, Vol 6, No 4, 2012, pp. 272-279.
 30. Jin, H., Hwang, M-O., Yoon, J., Lee, K., Chin, I-J., “Preparation and characterization of electrospun poly(L-lactic acid-co-succinic acid-co-1,4-butane

- diol) fibrous membranes”, *Macromolecular Research*, Vol. 13, No. 1, 2005, pp. 73-79.
31. Li, W., Danielson, K., Alexander, P., Tuan, R., “Biological response of chondrocytes cultured in three-dimensional nanofibers poly(ϵ -caprolactone) scaffolds”, *Journal of Biomedical Material Research*, Vol. 67A, No. 4, 2003, pp. 1105-1114.

